Lyme Disease Emergence after Invasion of the Blacklegged Tick, *Ixodes scapularis*, Ontario, Canada, 2010–2016

Manisha A. Kulkarni, Isha Narula, Andreea M. Slatculescu, Curtis Russell

Analysis of surveillance data for 2010–2016 in eastern Ontario, Canada, demonstrates the rapid northward spread of *Ixodes scapularis* ticks and *Borrelia burgdorferi*, followed by increasing human Lyme disease incidence. Most spread occurred during 2011–2013. Continued monitoring is essential to identify emerging risk areas in this region.

Lyme disease (LD) is the most reported vectorborne disease in North America, where it is caused by *Borrelia burgdorferi* sensu stricto and principally transmitted by the blacklegged tick (*Ixodes scapularis*) (*1*). With northward expansion of *I. scapularis* tick populations from endemic areas in the United States, LD is rapidly emerging in parts of central and eastern Canada (*2–4*). Although several studies have mapped blacklegged tick populations across Canada and developed models to predict future spread of ticks and LD risk (*2,3*), little is known about the extent of human LD in relation to tick vector distributions at a fine geographic scale. We examined spatiotemporal trends in the occurrence and expansion of *I. scapularis* ticks, *B. burgdorferi*–infected ticks, and human LD cases over a 7-year period to elucidate the process of LD emergence in eastern Ontario, Canada.

The Study

Our study included 3 public health units in eastern Ontario, Canada: Kingston, Frontenac, and Lennox and Addington (KFL); Leeds, Grenville, and Lanark (LGL); and Ottawa. This region spans from the St. Lawrence River in the south to the Ottawa River in the north, and has several major population centers, including Kingston (2016 population 123,798) and Ottawa (2016 population 934,243) (*5*). The region is largely characterized by mixed deciduous forest and agricultural land use.

We used data from the Integrated Public Health Information System database to identify human LD cases

Author affiliations: University of Ottawa, Ottawa, Ontario, Canada (M.A. Kulkarni, I. Narula, A.M. Slatculescu); Public Health Ontario, Toronto, Ontario (C. Russell)

on the basis of provincial case definitions (*6*). We geocoded cases to their forward sortation area (FSA) (i.e., first 3 digits of the postal code) of residence and extracted data on patient sex, age, episode date (onset of symptoms), and reported history of travel (defined as travel outside the municipality of residence within the previous 2 weeks). Data on ticks collected during 2010–2016 through passive tick surveillance activities in Ontario were obtained from Public Health Ontario (PHO) (*7*). We aggregated *I. scapularis* tick records according to the FSA of the submitter (i.e., location of residence of the person who acquired the tick) and excluded records with missing collection date, submitter FSA, or PCR test result and records with reported history of travel. We similarly excluded human LD records with missing patient FSA or with reported travel history. We obtained FSA-level population data for 2011 and FSA boundary files from Statistics Canada (*5*).

To examine the association between the invasion of *I. scapularis* ticks and *B. burgdorferi* and the spread of human LD, we examined associations between FSA-level data on time to first case (in years) and several variables: time to first reported *I. scapularis* tick, time to first reported *B. burgdorferi*–infected tick, distance to FSA with highest LD incidence in 2010, and population. We constructed bivariable and multivariable linear regression models with time to first case (in years) as the outcome.

To visualize LD spread during 2010–2016, we plotted the annual FSA-level incidence of human LD and *B. burgdorferi* prevalence in ticks by using ArcGIS 10.4 (ESRI, https://www.esri.com). We also assessed the annual weighted mean center and distribution of human LD incidence by using ArcGIS 10.4, after spatial projection of the data to preserve distance (*8*). We applied Kulldorff's spatial scan statistics (*9*) by using SaTScan 9.6 (https://www.satscan.org) to assess and compare spatiotemporal patterns in human LD incidence and *B. burgdorferi* prevalence in ticks at the FSA level (FSA centroids). (For additional methods, see the Appendix, https://wwwnc.cdc.gov/EID/article/25/2/18-0771-App1.pdf).

A higher proportion of LD cases occurred in men and in adults 50–69 years of age (Table 1), similar to patterns observed in other regions of North America (*10*). LD incidence increased over time; 55% of cases occurred during

Table 1. Incidence of Lyme disease and characteristics of 639 reported human Lyme disease case-patients in 3 public health units, eastern Ontario, Canada, 2010–2016*

Characteristic	No. (%) cases	Cumulative incidence, cases/100,000 population†	Mean (SD) annual incidence, cases/100,000 population†
Public health unit			
KFL	210 (33.0)	109.6	15.7 (13.3)
LGL	224 (35.1)	135.8	19.4 (10.4)
Ottawa	205 (32.1)	23.2	3.3 (2.8)
Total	639 (100.0)	51.5	7.4 (5.2)
Age group, y			
0–9	43 (6.7)	32.6	4.7 (4.5)
10–19	39 (6.1)	25.7	3.6 (2.2)
20–29	49 (7.7)	29.0	4.1 (3.3)
30–39	74 (11.6)	47.2	6.7 (4.2)
40–49	80 (12.5)	42.2	6.0 (5.0)
50–59	161 (25.2)	87.9	12.6 (8.5)
60–69	118 (18.5)	89.2	12.7 (9.9)
70–79	56 (8.8)	74.7	10.7 (8.8)
$\geq$80	19 (3.0)	38.1	5.4 (4.3)
Sex			
F	272 (42.6)	42.7	6.1 (4.5)
M	364 (57.0)	60.4	8.6 (6.1)
Data missing	3 (0.4)	–	–

*KFL, Kingston, Frontenac, Lennox, and Addington; LGL, Leeds, Grenville, and Lanark.
†Population based on 2011 census.

2015 and 2016 (Table 2). Roughly 70% of cases occurred during June–August, whereas $\approx$20% occurred during September–December. The number of collected ticks increased annually from 2010 and reached a peak in 2013, with a subsequent decrease because of reductions in passive surveillance activities in KFL and LGL (*11*); Ottawa received an increasing amount of ticks over time (Table 2). The percentage of ticks testing positive for *B. burgdorferi* increased annually, from 12% in 2010 to 23% in 2016 (p<0.001). Infection rates were higher among regions of KFL and LGL, although FSAs with high *B. burgdorferi* prevalence among submitted ticks were observed in parts of Ottawa in more recent years (Figure 1).

Within our study area, the first human LD case was reported an average of 2.2 years after the first reported *I. scapularis* tick and 1.1 years after the first reported *B. burgdorferi*–infected tick. Time to first case was significantly associated with time to first reported *I. scapularis* tick (adjusted $r^2 = 0.56$; p<0.001) and time to first *B. burgdorferi*–infected tick (adjusted $r^2 = 0.67$; p<0.001) after adjusting for distance to the FSA with highest LD incidence in 2010. The associated lag between each phase of $\approx$1 year supports the hypothesis that invasion and establishment of tick populations is followed by colonization of *B. burgdorferi* (*12*), or it might reflect the arrival of infected ticks with subsequent increase in *B. burgdorferi* prevalence. However, drawing conclusions on the exact timing of tick and pathogen invasion is difficult because of the nature of passive surveillance data.

LD incidence was concentrated in southern FSAs in 2010 and 2011 but had spread in a northeasterly direction by 2013 (Figure 2). Overall, a northeast shift of 54 km occurred between mean centers during 2010–2016, with the greatest spread observed in 2011–2013 (Appendix). We detected a spatiotemporal cluster of high rates of *B. burgdorferi*–infected ticks in the Kingston-Gananoque region bordering the St. Lawrence River, which overlapped with 2 clusters of human LD cases (Appendix Figure 4). The overlapping clusters support the conclusion that increased tick encounter is a determinant of human LD risk. Residence in endemic areas (i.e., where infected ticks

Table 2. Incidence of Lyme disease and number of *Ixodes scapularis* ticks submitted through passive tick surveillance, by year, 3 public health units, eastern Ontario, Canada, 2010–2016*

Characteristic and public health unit	2010	2011	2012	2013	2014	2015	2016
Incidence rate, cases/100,000 population†							
KFL	2.1	8.4	4.2	8.4	20.4	36.0	30.3
LGL	5.5	9.1	16.4	24.2	21.2	37.0	22.4
Ottawa	0.2	0.7	1.8	4.1	2.4	7.6	6.5
Total	1.2	3.0	4.1	7.4	7.7	15.9	12.3
No. Ixodes scapularis tick submissions							
KFL	209	620	677	864	115	51	23
LGL	359	865	870	969	468	69	17
Ottawa	38	106	134	239	258	216	336
Total	606	1,591	1,681	2,072	841	336	386

*KFL, Kingston, Frontenac, Lennox, and Addington; LGL, Leeds, Grenville, and Lanark.
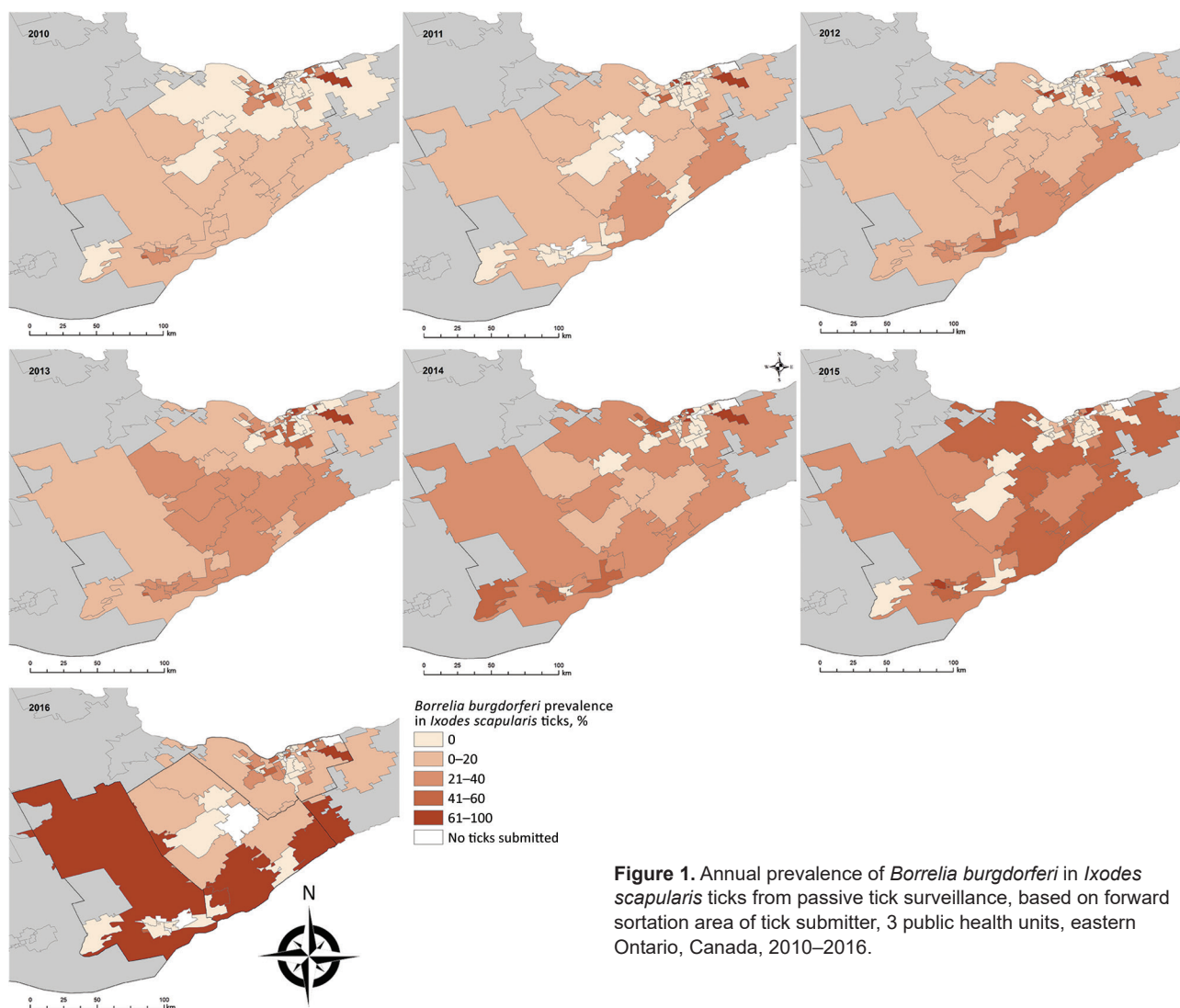†Population based on 2011 census.

Figure 1. Annual prevalence of *Borrelia burgdorferi* in *Ixodes scapularis* ticks from passive tick surveillance, based on forward sortation area of tick submitter, 3 public health units, eastern Ontario, Canada, 2010–2016.

have been found) has been consistently recognized as a risk factor for LD infection (*13,14*).

Conclusions

Although LD incidence in Ottawa had reached ≈7 cases/100,000 population by 2015–2016, the observed incidence rates in KFL and LGL during this period were 4-fold higher (≈30 cases/100,000 population). By comparison, these rates are still far below the ≈110 cases/100,000 population observed in the bordering St. Lawrence County of New York state (*15*). Given the ongoing emergence process, LD incidence will likely continue to increase in eastern Ontario as *I. scapularis* tick populations and *B. burgdorferi* continue to establish and fill in suitable habitats (*12*). This pattern highlights the importance of fine-scale studies to identify patterns and determinants of LD and other tickborne pathogens in different regions and populations.

Our study was limited by the availability of information on location of tick acquisition and patient exposure location. As such, we aggregated data at the FSA level on the basis of location of patient and tick submitter residence and excluded case-patients and tick submitters with reported travel outside their municipality of residence. Spatiotemporal analysis based on the location of exposure would help to more precisely determine the timing and rate of spread.

Altogether, our findings indicate that LD has emerged in eastern Ontario over a relatively short timescale after the invasion of *I. scapularis* ticks and *B. burgdorferi*. Tick surveillance data can serve to identify areas of risk for LD emergence.
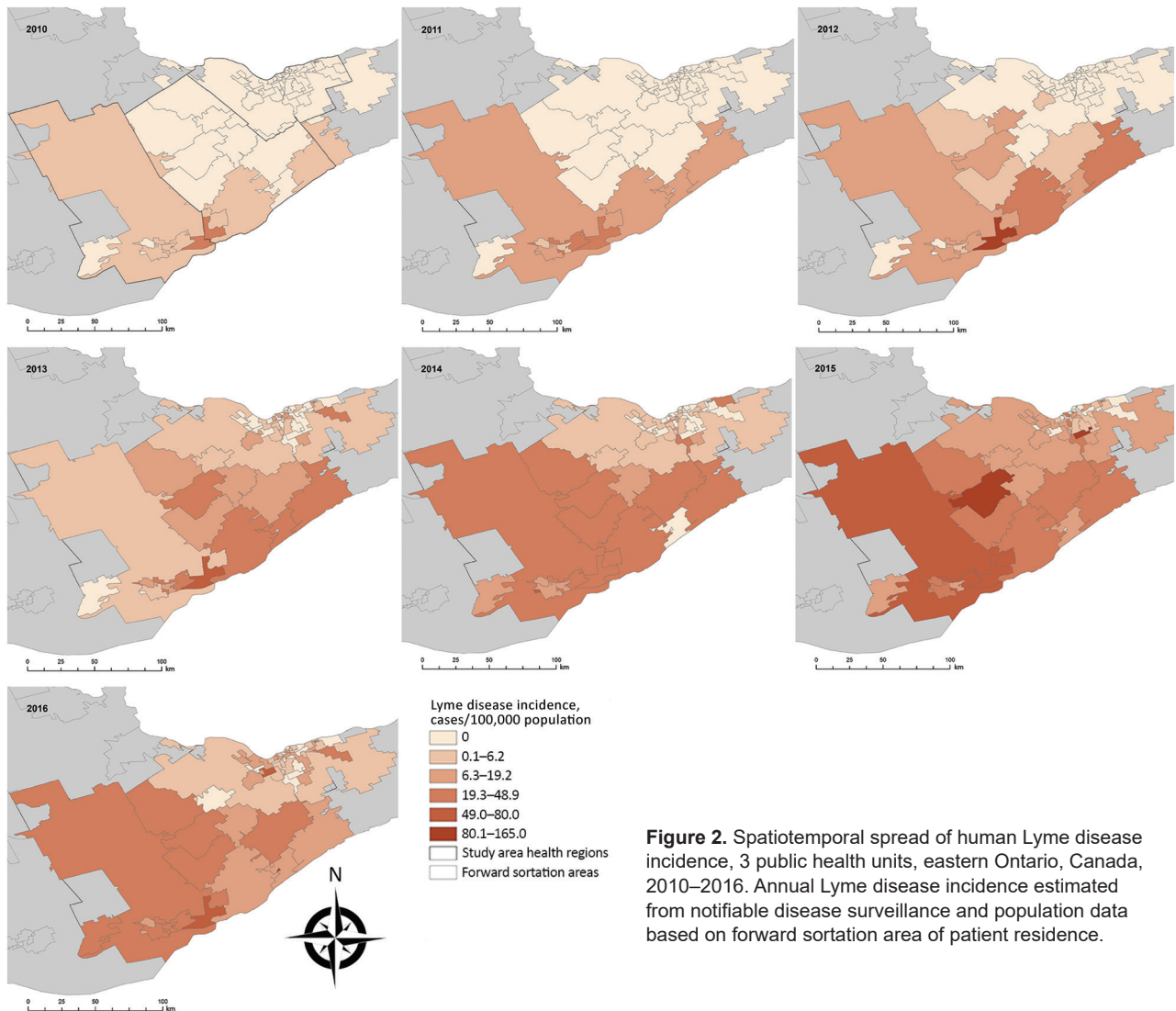
Acknowledgments

Figure 2. Spatiotemporal spread of human Lyme disease incidence, 3 public health units, eastern Ontario, Canada, 2010–2016. Annual Lyme disease incidence estimated from notifiable disease surveillance and population data based on forward sortation area of patient residence.

Legend: Lyme disease incidence, cases/100,000 population
- 0
- 0.1–6.2
- 6.3–19.2
- 19.3–48.9
- 49.0–80.0
- 80.1–165.0
- Study area health regions
- Forward sortation areas

About the Author

Dr. Kulkarni is a medical entomologist and assistant professor in the School of Epidemiology and Public Health at the University of Ottawa. Her research interests include vectorborne diseases with a focus on mosquitoborne and tickborne diseases in Canada and sub-Saharan Africa.

References

1. Bacon RM, Kugeler KJ, Mead PS; Centers for Disease Control and Prevention (CDC). Surveillance for Lyme disease—United States, 1992–2006. MMWR Surveill Summ. 2008;57:1–9.
2. Ogden NH, Bouchard C, Kurtenbach K, Margos G, Lindsay LR, Trudel L, et al. Active and passive surveillance and phylogenetic analysis of *Borrelia burgdorferi* elucidate the process of Lyme disease risk emergence in Canada. Environ Health Perspect. 2010;118:909–14. http://dx.doi.org/10.1289/ehp.0901766
3. Ogden NH, St-Onge L, Barker IK, Brazeau S, Bigras-Poulin M, Charron DF, et al. Risk maps for range expansion of the Lyme disease vector, *Ixodes scapularis*, in Canada now and with climate change. Int J Health Geogr. 2008;7:24. http://dx.doi.org/10.1186/1476-072X-7-24
4. Ogden NH, Lindsay LR, Morshed M, Sockett PN, Artsob H. The emergence of Lyme disease in Canada. CMAJ. 2009;180:1221–4. http://dx.doi.org/10.1503/cmaj.080148

5. Statistics Canada. Focus on Geography Series, 2016 census. Statistics Canada catalogue no. 98–404–X2016001. Ottawa (Ontario, Canada): Statistics Canada; 2017.

6. Ministry of Health and Long-Term Care. Infectious disease protocol appendix B: provincial case definitions for reportable diseases. Toronto (Ontario, Canada): Ministry of Health and Long-Term Care; 2017.

7. Nelder MP, Russell C, Lindsay LR, Dhar B, Patel SN, Johnson S, et al. Population-based passive tick surveillance and detection of expanding foci of blacklegged ticks *Ixodes scapularis* and the Lyme disease agent *Borrelia burgdorferi* in Ontario, Canada. PLoS One. 2014;9:e105358. http://dx.doi.org/10.1371/journal.pone.0105358

8. Mitchell A. The ESRI guide to GIS analysis. Vol. 2. Redlands (CA, USA): ESRI; 2005.

9. Kulldorff M. A spatial scan statistic. Commun Stat Theory Methods. 1997;26:1481–96. http://dx.doi.org/10.1080/03610929708831995

10. Schwartz AM, Hinckley AF, Mead PS, Hook SA, Kugeler KJ. Surveillance for Lyme disease—United States, 2008–2015. MMWR Surveill Summ. 2017;66:1–12. http://dx.doi.org/10.15585/mmwr.ss6622a1

11. Ontario Agency for Health Protection and Promotion. Technical report: update on Lyme disease prevention and control. Toronto (Ontario, Canada): Ontario Agency for Health Protection and Promotion; 2016.

12. Clow KM, Leighton PA, Ogden NH, Lindsay LR, Michel P, Pearl DL, et al. Northward range expansion of *Ixodes scapularis* evident over a short timescale in Ontario, Canada. Wooten RM, editor. PLoS One. 2017;12:e0189393.

13. Cromley EK, Cartter ML, Mrozinski RD, Ertel S-H. Residential setting as a risk factor for Lyme disease in a hyperendemic region. Am J Epidemiol. 1998;147:472–7. http://dx.doi.org/10.1093/oxfordjournals.aje.a009473

14. Finch C, Al-Damluji MS, Krause PJ, Niccolai L, Steeves T, O'Keefe CF, et al. Integrated assessment of behavioral and environmental risk factors for Lyme disease infection on Block Island, Rhode Island. PLoS One. 2014;9:e84758. http://dx.doi.org/10.1371/journal.pone.0084758

15. New York State Department of Health. Lyme disease incidence per 100,000. Bureau of Communicable Disease Control Data 2013–2015. New York: New York State Department of Health; 2017.

Address for correspondence: Manisha A. Kulkarni, University of Ottawa Faculty of Medicine, School of Epidemiology and Public Health, 600 Peter Morand Crescent, Ottawa, ON K1G 5Z3, Canada; email: manisha.kulkarni@uottawa.ca

Lyme Disease Emergence after Invasion of the Blacklegged Tick, *Ixodes scapularis*, Ontario, Canada, 2010–2016

Appendix

Supplementary Methods

Data Sources

Reportable Disease Surveillance Data

All public health units (PHUs) in Ontario are required to collect and report information on patients with reportable diseases to the Ministry of Health and Long-Term Care (MOHLTC). This information is entered into the Integrated Public Health Information System (iPHIS) database and used for local, provincial, and national surveillance. A map of the three PHUs included in the study is shown in Supplementary Figure 1. We defined cases as patients with confirmed or probable Lyme disease (LD) as defined by MOHLTC (*1*).

Tick Surveillance Data

Passive tick surveillance involves the voluntary submission of ticks by the public and by physicians and veterinarians from patients. Public Health Ontario (PHO) receives and identifies ticks that have been found on human hosts and submitted from public health units and/or directly from healthcare providers; these data are then collated with real-time polymerase chain reaction (PCR) test results from the National Microbiology Lab (*2*).

Statistical Analysis

We completed all statistical analyses using Stata 15; a two-sided significance level of 5% was used for statistical testing. We calculated LD incidence rates as the total annual number of cases in a given FSA divided by the FSA population. Similarly, we calculated annual *B. burgdorferi* prevalence as the total number of submitted *I. scapularis* ticks with positive real-

time PCR results for *B. burgdorferi* divided by the total number of ticks that were tested in a given FSA and year.

To examine the association between the invasion of *I. scapularis* and *B. burgdorferi* and the spread of human LD, we examined bivariable associations between FSA-level data on time to first case (in years) and the following independent variables: time to first reported *I. scapularis* tick, time to first reported *B. burgdorferi*-infected tick, distance to origin, and population. We constructed linear regression models with time to first case (in years) as the outcome and variables that were significant in bivariable analyses as predictors. The origin of LD was defined as the FSA with highest LD incidence in 2010, which corresponded to the town of Gananoque. We tested data for linearity and normality and examined model residuals to test goodness of fit.

Spatial Analysis

To visualize LD spread from 2010 to 2016, we plotted the annual FSA-level incidence of human LD and *B. burgdorferi* prevalence in ticks using ArcGIS v10.4. We excluded tick records with missing collection date, patient FSA, PCR test result, and records with reported history of travel. Similarly, we excluded human LD records with missing patient residence information or with a reported history of travel. We assessed the annual weighted mean center and directional distribution of human LD incidence using the spatial analyst extension in ArcGIS, following spatial projection of the data to preserve distance (*3*). The resulting weighted mean center location represents the geographic center of concentration of features (FSA centroids) weighted by annual rates, while the deviation ellipses indicate 1 SD of the geographic mean annual incidence, calculated as the incidence weighted average in space for each FSA, with incidence attributed to the FSA centroid.

Cluster Analysis

We applied Kulldorf's spatial scan statistics (*4*) to assess and compare spatiotemporal patterns in human LD incidence and *B. burgdorferi* prevalence in ticks at the FSA level (FSA centroids). We used a Poisson-based probability model to detect space-time clusters of human LD cases occurring over FSAs in the three PHUs, adjusting for FSA population size. We used a Bernoulli-based probability model to detect clusters of *B. burgdorferi* infected ticks, with infected and non-infected ticks representing cases and controls, respectively. Using SaTScanTM, we set the scan to detect clusters with high rates, with 10% or 50% maximum spatial cluster size

for human cases and ticks, respectively, and with a 1-year minimum temporal window size. Significance of clusters was based on 999 Monte Carlo replications using a p-value of <0.05.

Supplementary Results

Epidemiology of LD

From 2010 to 2016, there were a total of 762 reported cases of LD within the study area. Of these, we excluded 123 from the analysis based on a reported history of travel. Of the 639 cases that were retained, we observed a higher proportion among males (n = 364, 57.0%) than females (n = 272, 42.6%). Cases ranged in age from under 1 year to 93 years (mean = 47.1 years of age; SD±20.4) with a peak among adults aged 45–69 years. Despite similar total case numbers among the three health units, incidence rates were higher in KFL and LGL owing to their lower overall population (Supplementary Figure 2).

Among all FSAs in the study area, the first human LD case was reported an average of 2.0 years following the first reported *I. scapularis* tick, and 0.6 years following the first reported infected tick. However, two FSAs reported human cases before any *I. scapularis* ticks were detected through passive surveillance, and six FSAs reported human cases before detection of *B. burgdorferi* in submitted ticks. This discrepancy may be due to differences in sensitivity of tick surveillance or may reflect patient exposure outside of the FSA of residence, despite our restriction based on travel history. We conducted a sensitivity analysis excluding discrepant FSAs (i.e., FSAs with human cases reported before a signal from tick surveillance), and found 2.2 and 1.1 years respectively following the first reported tick or *B. burgdorferi*-infected tick.

In bivariable analyses, time to first human LD case (in years) was independently associated with time to first *I. scapularis* tick ($r2 = 0.35$, $p < 0.001$), time to first *B. burgdorferi*-infected tick ($r2 = 0.61$, $p < 0.001$) and distance to origin ($r2 = 0.46$, $p < 0.001$), but not population size ($p = 0.062$). Time to first tick and time to first *B. burgdorferi* infected tick were highly correlated (Spearman rank correlation 0.78), therefore separate models were fit for each predictor. In a multivariable regression, after adjusting for distance to origin, time to first case was significantly associated with time to first reported *I. scapularis* tick (adjusted $r2 = 0.56$, $p < 0.001$). Time to first *B. burgdorferi*-infected tick was also strongly associated with time to first human LD case after controlling for distance from origin (adjusted $r2 = 0.67$, $p < 0.001$).

Trends in Tick Surveillance

A total of 7760 *I. scapularis* ticks were recorded from 2010 to 2016 through passive surveillance activities in the study area. Of these, 233 of submitters reported recent travel (95 outside of Canada and 138 within Canada); we excluded these records from analysis. Of the 7527 ticks retained in analyses, almost half were submitted by individuals residing in LGL (n = 3617, 48.2%), followed by KFL (n = 2559, 34.1%) and OTT (n = 1395, 17.7%). The number of collected ticks increased annually until 2014, when KFL and LGL no longer accepted tick submissions from the public (although healthcare providers could still submit ticks to PHO). Ticks were received throughout the entire year, with bimodal peaks from April to June and October to November reflecting the submission of mainly adult ticks, which are easier to see and more likely to be submitted than nymphal ticks.

Of the 5753 ticks with real-time PCR results for *B. burgdorferi*, 1209 (21.0%) tested positive; 1774 records had no test results reflecting ticks that were not forwarded for testing due to damage or poor specimen condition. The overall (cumulative) *B. burgdorferi* prevalence in ticks was similar among health units, with 21.6%, 21.0%, and 19.5% prevalence in KFL, LGL, and OTT, respectively. There was a significant association between infection status (positive/negative) and year of tick submission (p < 0.001).

Spatial and Cluster Analysis

We excluded 45 cases due to missing patient residence information and retained 594 human cases in spatial analyses. Deviational ellipses depict the spatiotemporal trend in LD incidence, which was concentrated in southern FSAs in 2010 and 2011 but had spread in a northeasterly direction by 2013 (Supplementary Figure 3). The directional trend was consistent from 2013 to 2016 reflecting the occurrence of reported LD cases in OTT from 2013 onward. Distances between mean centers, reflecting the change in LD distribution from year to year, increased from 2010 to 2013: 4.3 km (2010 to 2011), 20.9 km (2011 to 2012) and 35.8 km (2012 to 2013) (mean 20.3 km/year) and stabilized thereafter. Overall, a northeast shift of 54 km was observed between mean centers from 2010 to 2016.

We excluded 706 tick records with missing submitter residence information and retained 5047 records in spatial analysis; 1068 (21.1%) were positive for *B. burgdorferi*.

Space-time Poisson analysis revealed six clusters of high human LD incidence, two of which were significant (p < 0.001). The first significant cluster of human infection was 66 km in radius, was composed of 3 FSAs (including one geographically large FSA in KFL) covering a population of 93,811 and occurred over the period from 2014 to 2016. The incidence of LD within the cluster was 42.6 per 100,000, with a relative risk of 7.9. The second significant cluster of human infection centered on the Kingston-Gananoque region was 32 km in radius, was composed of 5 FSAs covering a population of 126,827, and also occurred over the period from 2014 to 2016. The incidence of LD within the cluster was 26.8 per 100,000, with a relative risk of 4.7. A similar pattern was observed in the space-time Bernouilli model, which revealed seven clusters of high rates of *B. burgdorferi* infected ticks, with one significant cluster (p < 0.0001). The significant cluster was 77 km in radius spanning 9 FSAs and overlapping spatially with the clusters of human LD cases. The infected tick cluster contained 28.5% of all infected ticks with RR = 1.6, and was observed over the period 2012 to 2014.

References

1. Ministry of Health and Long-Term Care. Infectious disease protocol appendix B: provincial case definitions for reportable diseases. Toronto: Ministry of Health and Long-Term Care; 2017.

2. Nelder MP, Russell C, Lindsay LR, Dhar B, Patel SN, Johnson S, et al. Population-based passive tick surveillance and detection of expanding foci of blacklegged ticks *Ixodes scapularis* and the Lyme disease agent *Borrelia burgdorferi* in Ontario, Canada. PLoS One. 2014;9:e105358. PubMed http://dx.doi.org/10.1371/journal.pone.0105358

3. Mitchell A. The ESRI guide to GIS analysis. Vol. 2. Redlands (California): ESRI; 2005.

4. Costa MA. Kulldorf M. Applications of spatial scan statistics: a review. In: Scan statistics: methods and applications. Boston: Birkhäuser]; 2009. p. 129–52.
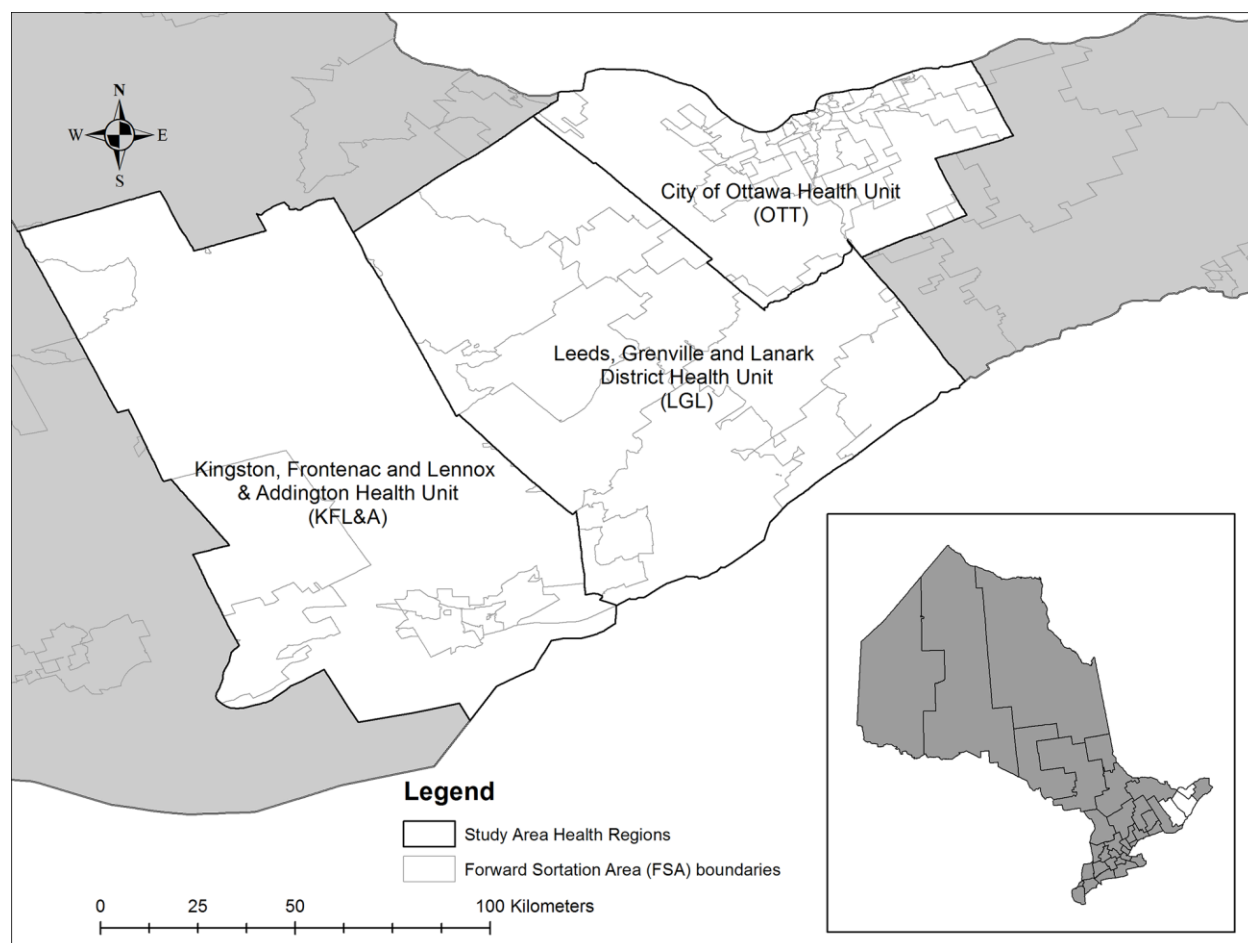
Appendix Figure 1. Map of study area showing three public health units in eastern Ontario, Canada. Inset map shows the province of Ontario with the study area location in white.
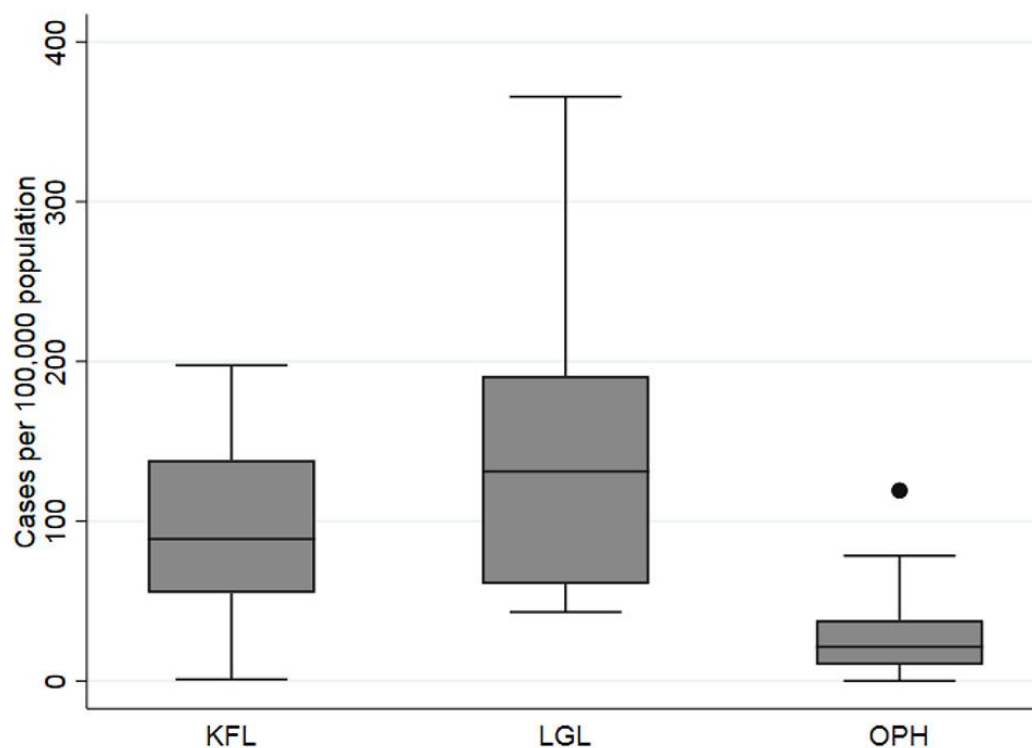
Appendix Figure 2. Boxplot of cumulative Lyme disease incidence, 2010–2016, in three eastern Ontario public health units. Error bars show 95% confidence intervals and point indicates outlier data, based on data from forward sortation areas in each health unit; Kingston, Frontenac, Lennox & Addington (KFL), Leeds, Grenville, Lanark (LGL), Ottawa (OTT).
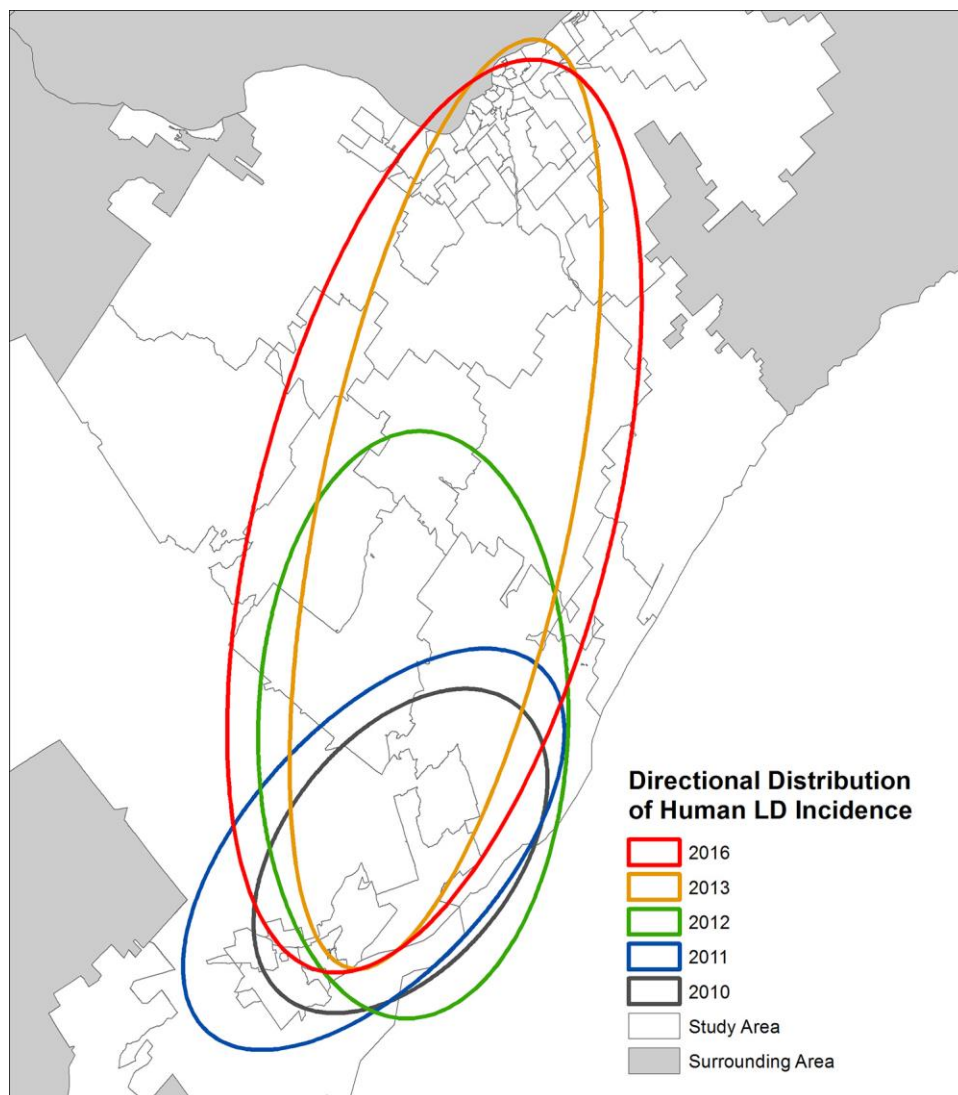
Appendix Figure 3. Deviational ellipses indicating the directional distribution of human Lyme disease incidence in three eastern Ontario public health units, 2010–2016.

Appendix Figure 4. Spatiotemporal clusters of high rates of *Borrelia burgdorferi*–infected ticks (dark blue outline) and human Lyme disease cases (yellow and red outlines) in three eastern Ontario public health units, 2010–2016. The relative risk (RR) and duration of observed clusters (start and end year) are indicated in the figure legend.